International Journal of Bifurcation and Chaos, Vol. 19, No. 8 (2009) 2801–2812

DYNAMICS OF AN INTERFACE CONNECTING A STRIPE PATTERN AND A UNIFORM STATE: AMENDED NEWELL–WHITEHEAD–SEGEL EQUATION

RENÉ G. ROJAS*, RICARDO G. ELÍAS and MARCEL G. CLERC
Departamento de Física,
Facultad de Ciencias Físicas y Matemáticas,
Universidad de Chile, Casilla 487-3, Santiago, Chile
**Instituto de Física, Pontificia Universidad Católica de Valparaíso,*
Casilla 4059, Valparaiso, Chile

Received April 19, 2008; Revised October 2, 2008

The dynamics of an interface connecting a stationary stripe pattern with a homogeneous state is studied. The conventional approach which describes this interface, Newell–Whitehead–Segel amplitude equation, does not account for the rich dynamics exhibited by these interfaces. By amending this amplitude equation with a nonresonate term, we can describe this interface and its dynamics in a unified manner. This model exhibits a rich and complex transversal dynamics at the interface, including front propagations, transversal patterns, locking phenomenon, and transversal localized structures.

Keywords: Amplitude equations; interface dynamics; localized structures.

1. Introduction

Nonequilibrium systems are commonly exhibited as equilibrium extended states: uniform, oscilatory, chaotic, and pattern states [Nicolis & Prigogine, 1977]. By changing the parameters, a uniform state can bifurcate to a pattern state, the system under study has a *spatial bifurcation*. This instability arises when a control parameter exceeds a critical value. The difference between the control parameter and the critical value is usually called the bifurcation parameter [Nicolis & Prigogine, 1977]. Often, the macroscopical or mesoscopical equations that govern the dynamical behavior of the system under study are complicated and do not have analytical solutions available; nevertheless, close to the instability threshold, the system can be well described by a set of equations called *amplitude equations* [Landau, 1944; Stuart, 1960; Schlüter *et al.*, 1965]. These equations describe the dynamical behaviors of the amplitude for the critical modes. The relation of the amplitudes with the initial physical variables is given by an asymptotic series close to the identity [Elphick *et al.*, 1987]. Amplitude equations are valid for weak nonlinearities, and slow modulations in space and time. These models successfully describe a large number of patterns forming in: Rayleigh–Benard convection, Taylor–Couette flow, Faraday instability, directional solidification, nonlinear optics, chemical reactions, biological systems, and so forth [Cross & Hohenberg, 1993; Newell *et al.*, 1993; van Hecke *et al.*, 1994]. However, there are several phenomena which are not described by amplitude equations, e.g. the nonadiabatic effects such as the pinning range [Pomeau, 1986; Aranson *et al.*, 2000], localized patterns [van Saarloos & Hohenberg, 1992; Sakaguchi & Brand, 1996], interface dynamics in a two-dimensional system [Malomed *et al.*, 1990; Hagberg *et al.*, 2006; Burke & Knobloch, 2007; Clerc *et al.*, 2008], noise induces propagation [Clerc *et al.*, 2005b], and localized peaks

[Bortolozzo *et al.*, 2005, 2006]. One way to take into account these phenomena is to include the nonresonant terms in the amplitude equations [Bensimon *et al.*, 1988; Clerc & Falcon, 2005; Clerc *et al.*, 2005b]. Another way to describe these phenomena is going beyond all orders of the usual multiple-scale expansion [Kozyreff & Chapman, 2006]. All these phenomena are not described by the conventional amplitude equations approach and they are a consequence of the interaction of the spatial variation of the envelope or amplitude with the underlying pattern.

One of the most well-known amplitude equations in two-dimensional systems is the *Newell–Whitehead–Segel equation* (NWS) [Segel, 1969; Newell & Whitehead, 1969; 1971]. This model describes the appearance of the stripe pattern in two-dimensional systems, and their respective secondary instabilities like Eckhaus, and zigzag [Jakobsen *et al.*, 1994; Walgraef, 1996]. However this amplitude equation does not take into account the transversal dynamics of the interface connecting a stripe pattern with a uniform state [Hagberg *et al.*, 2006; Clerc *et al.*, 2008]. In particular, the depinning effect has been reported between a stripe pattern and a uniform state in the supercritical Swift–Hohenberg model [Hagberg *et al.*, 2006]. In this system the flat interface presents a spatial instability followed by nucleation of convex–concave disclination pairs and finally the system displays a labyrinthic pattern. Hence, the nonlinear response in this model does not saturate the instability and does not give rise to coarsening process. On the contrary, numerical simulations in the subcritical Swift–Hohemberg equation show that this interface has transversal spatial periodic structures, zigzag dynamics and complex coarsening process [Burke & Knobloch, 2007; Clerc *et al.*, 2008]. In the last decade, interface dynamics has attracted attention to different fields of science, including biology, chemistry, and physics [Murray, 1993]. Most of these studies of an interface between patterns and homogeneous states have been developed in one-dimensional systems. However, in two dimensions few studies have been performed of the interface connecting pattern states to uniform ones.

The aim of this manuscript is to study the dynamics of an interface connecting a stripe pattern with an homogeneous one. To describe in a unified manner this type of interface we consider the amended NWS equations, that is NWS with extra nonresonant terms. Since, the conventional NWS does not describe the wealthy interface dynamics observed in a prototype model, which has interfaces with a stripe pattern and a uniform state, we show that amending the NWS equation, one can render and recover the rich and complex transversal dynamics at the interface, including interface or front propagation, transversal spatial pattern (which has been recently termed *embroidery* [Clerc *et al.*, 2008]), locking phenomena, and transversal localized structures.

The manuscript is organized as follows: In Sec. 2 the NWS equation is introduced, the generalization of this model is presented in Sec. 3. The transversal interface dynamics is described in Sec. 4. The localized structures observed in the transversal interface are discussed in Sec. 5, and conclusions and remarks are presented in Sec. 6.

2. The Newell–Whitehead–Segel Equation

Let us consider a two-dimensional isotropic dynamical system with a homogeneous solution $\mathbf{u}(x, y, t) = \mathbf{u}_o$

$$\partial_t \mathbf{u} = \mathbf{F}(\mathbf{u}, \partial_x, \partial_y, \{\lambda\}), \quad \mathbf{F}(\mathbf{u}_o, \partial_x, \partial_y, \{\lambda\}) = 0, \tag{1}$$

where $\mathbf{u}(x, t)$ is a field of dimension n that describes the system under study, $\mathbf{F}$ is the vector field which accounts for the dynamics of the system, the symbols ∂_x, ∂_y and ∂_t stand for derivatives with respect to the x, y and t variables, respectively. $\{\lambda\}$ is a set of parameters which characterize the system under study. In order to study the interface connecting a stripe pattern with a uniform state, the dynamical system (1) needs to exhibit coexistence between a stationary stripe pattern and a homogeneous state. A simple way to have this scenario is that the system (1) has a subcritical or inverted bifurcation at a finite spatial wave length. From the point of view of dynamical system theory, this type of bifurcation is generic, however a few physical examples are known in two extended dimensions such as Rayleigh–Benard in binary fluids [Burke & Knobloch, 2006]. When the dynamical system (1) is isotropic, and for the sake of simplicity we choose the direction of variation of the stripes as the x-direction, then close to the spatial bifurcation one can propose as solution [Cross & Hohenberg, 1993]

$$\mathbf{u} = \mathbf{u}_o + [A(x, y, t)\, e^{iqx} + \overline{A}(x, y, t)\, e^{-iqx}]\, \hat{v} + \sum_{n,m} a_{nm} A^n \overline{A}^m\, e^{i(n-m)qx} \hat{u}_{nm}, \tag{2}$$

where $\hat{v}$ is the growing direction of the marginal mode with wave number $\mathbf{q} = (q, 0)$ and $A(x, y, t)$ is the envelope or amplitude of the critical mode $e^{iqx}\hat{v}$. Introducing the above ansatz in Eq. (1) after straightforward calculation one arrives at the dimensionless subcritical Newell–Whitehead–Segel equation (NWS)

$$\partial_t A = \epsilon A + \nu|A|^2 A - |A|^4 A + \left(\partial_x - i\frac{2}{q}\partial_{yy}\right)^2 A, \tag{3}$$

where ϵ is the bifurcation parameter, for negative (positive) ϵ the uniform state u_o is stable (unstable). The parameter ν controls the type of bifurcation (super and subcritical). Positive ν accounts for a subcritical bifurcation. Hence, below the bifurcation the uniform state u_o is stable, by increasing the bifurcation parameters, this state becomes unstable and gives rise to a stripe pattern with finite amplitude. Decreasing the bifurcation parameter ($\epsilon < 0$ and $\nu > 0$) the amplitude of stripe pattern decreases and this solution coexists with the uniform state, which correspond to the coexisting region. Higher-order terms are ruled out by the following scaling, $\nu \sim \epsilon^{1/2}$, $|A| \sim \epsilon^{1/4}$, $\partial_t \sim \epsilon$, $\partial_x \sim \epsilon^{1/2}$, $\partial_y \sim \epsilon^{1/4}$ and $\epsilon \ll 1$. Hence, the above equation is of order $\epsilon^{3/2}$. For the sake of simplicity and without loss of generality rescaling time, space, the amplitude A, and fixing $\nu = 1$, the amplitude equation reads

$$\partial_t A = \epsilon A + |A|^2 A - |A|^4 A + \left(\partial_x - i\frac{2}{q}\partial_{yy}\right)^2 A. \tag{4}$$

Due to the isotropy property of the original system, Eq. (1), the spatial operator in the NWS Eq. (4) is anisotropic because perturbations in the direction of the stripes are not equal to those in the orthogonal direction. Notice that the above model (4) is variational, i.e.

$$\partial_t A = -\frac{\delta \mathcal{F}}{\delta \overline{A}}, \tag{5}$$

where

$$\mathcal{F} = \int \left(-\epsilon|A|^2 - \frac{|A|^4}{2} + \frac{|A|^6}{3} + \left|\left(\partial_x - \frac{i2}{q}\partial_{yy}\right) A\right|^2\right) dxdy. \tag{6}$$

Hence, the dynamics of the amplitude equation (4) is characterized by the minimization of this functional $\mathcal{F}$. This functional has two trivial equilibria states $A_o = 0$ and $A_1 = (1/2 + \sqrt{\epsilon + 1/4})^{1/2} e^{i\phi}$ where ϕ is an arbitrary constant. This equation has a family of front solutions connecting the homogeneous states A_o and A_1. The solutions A_o and A_1 represent the homogeneous and the spatial periodic states of the original dynamical system, respectively. This front is static only at the *Maxwell point* [Goldstein *et al.*, 1990], i.e. for $\epsilon_M = -3/16$. For $\epsilon < \epsilon_M$ the homogeneous solution invades the periodic one and for $\epsilon > \epsilon_M$ the periodic invades the homogeneous state because the most favorable state — that is the global minimum of $\mathcal{F}$ — invades

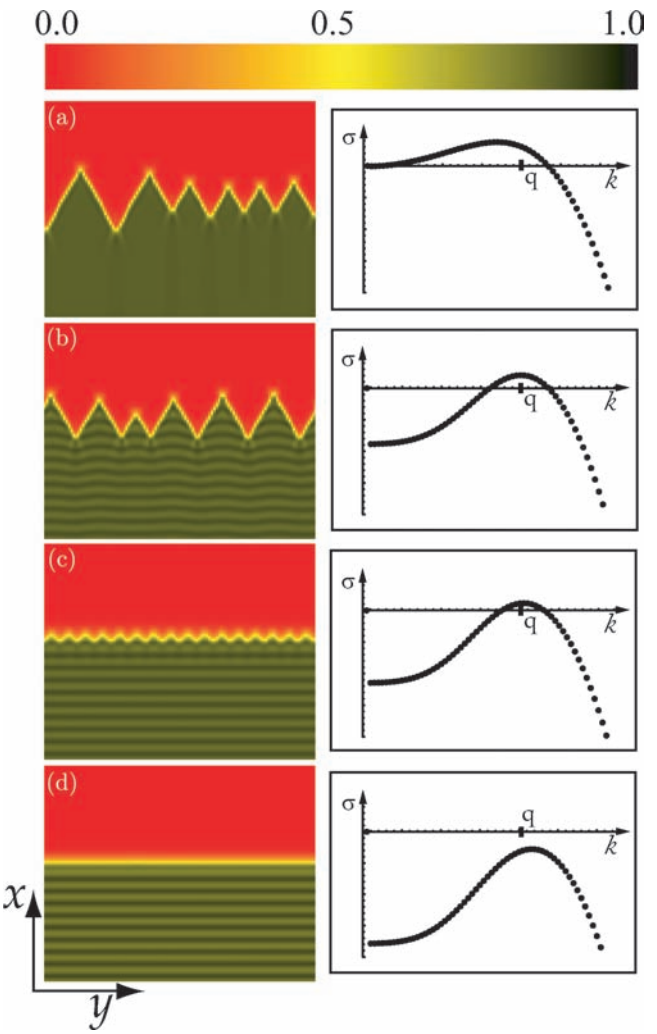

Fig. 1. Density plot of $|A|$ of model (9) with $\epsilon = -3/16$, $q = 2.6$, and for: (a) $\eta = 0.0$, (b) $\eta = 0.08$, (c) $\eta = 0.10$, and (d) $\eta = 0.15$. The figures on the right are the linear spectra of the flat interface respectively. The inset figures (a) and (b) depict the typical coarsening dynamics exhibited by model (3) and the inset figures (c) and (d) are the final states observed in the respective regime of the parameter. On top, we give the scale of all density plots.

the other. At the Maxwell point, the front solution is motionless and has the form

$$A(x,y) = \sqrt{\frac{\frac{3}{4}}{1+e^{\pm\sqrt{3/4}(x-P)}}}\, e^{i\theta}, \tag{7}$$

where P is the position of the interface, and θ is an arbitrary phase. Hence, the family of front solutions is parameterized by two continuous parameters $\{P,\theta\}$. From now on, we will denominate core or interface of the front, the region of the space where the front solution has a large spatial variation. Numerical simulations show that this front interface is unstable in the transversal direction (y-direction). Numerically, we have computed the growth rate of the transversal mode of the interface [cf. Fig. 1(a)]. The most unstable transversal mode, has a wave number close to the original critical one q.

In [Sakaguchi & Brand, 1996], an interface is shown that connects a stripe pattern with an uniform state exhibiting a locking phenomenon in the context of quintic Swift–Hohenberg equation. More recently in [Clerc *et al.*, 2008] is shown that these interfaces can suffer a transversal spatial instability, which gives rise to transversal patterns (embroideries), and nonlinear zigzag dynamics. The NWS model (4) cannot render account of these phenomena, because it does not exhibit locking phenomenon and embroideries at the interface. In the next section, we will present a formalism which allows to recover the dynamics exhibited by the original system.

3. The Amended Amplitude Equation

To describe the observed phenomena, we propose to amend the NWS equation, i.e. to consider the nonresonant terms in the conventional amplitude equation. Below the bifurcation, the equilibrium state has the continuous symmetry $x \to x+\alpha$, but above the bifurcation this symmetry is spontaneously broken by the stripe pattern. The ansatz (2) shows that, above the bifurcation, the system has the symmetry $x \to x+\alpha$ and $A \to A\,e^{iq\alpha}$, simultaneously. However, the NWS equation (4) possesses this symmetry independently. In order to restore the spatial symmetry of the original system, we consider the nonresonant terms in the amplitude equation, which reads

$$\partial_t A = \epsilon A + |A|^2 A - |A|^4 A + \left[\partial_x - i\frac{2}{q}\partial_{yy}\right]^2 A + \sum_{m,n} c_{mn} A^m \overline{A}^n e^{i(m-n-1)qx}, \tag{8}$$

where $m-n \neq 1$ and c_{mn} are coefficients of order one. All these extra terms are usually neglected, because they represent rapidly varying spatial oscillations, that is, these terms are exponentially small in the scaling under consideration. However, these terms are invariants under the transformation $x \to x-\alpha$ and $A \to A\,e^{iq\alpha}$ and then they restore the right symmetry of the amplitude equation. For a system with reflection symmetry one needs to consider that the extra condition $m+n$ is a odd number. To explore the effects of restoring the original spatial symmetry and for the sake of simplicity we consider the dominating term of the nonresonant terms for a system with reflexion symmetry, that is, $m=3$ and $n=0$, then *the Amended Newell–Whitehead–Segel equation* (ANWS), reads

$$\partial_t A = \epsilon A + |A|^2 A - |A|^4 A + \left[\partial_x - i\frac{2}{q}\partial_{yy}\right]^2 A + \eta A^3 e^{i2qx} \tag{9}$$

where η is the intensity of the spatial forcing or the nonresonant term, and without loss of generality it is taken to be positive as a result of the symmetry $\eta \to -\eta$ and $x \to x+\pi/(2q)$ of the above model. This equation has three other symmetries: $x \to -x$ and $A \to \overline{A}$ simultaneously, $A \to -A$, and $y \to -y$. Notice that the nonresonant term is a spatial forcing term with amplitude η and frequency $2q$. Hence, one expects the non-null uniform state to become a spatial periodic state.

For $\epsilon = \epsilon_M = -3/16$ — Maxwell's point — and $\eta = 0.0$, the front (7) is stationary, linearly unstable in the transversal direction and it develops a zigzag instability without a characteristic length scale. Figure 1(a) shows the growth rate of transversal mode as a function of the wave number. Hence, the most unstable mode has a wave number close to q; the modes with large (small) wave number are stable (unstable). Initially, the interface develops an spatial instability characterized by a well-defined wavelength, which is close to $2\pi/q$ and gives rise to sinusoidal interface. Later on, the sinusoidal shape of the interface becomes a zigzag interface [cf. Fig. 1(a)]. Two adjacent pieces of the zigzag

interface, whose orientations are opposite, are connected by a region of strong curvature which is usually denominated *kink* [Chevallard *et al.*, 2002]. The dynamics of interface consists then in reassembling domains of even orientation. It is important to note that the angle of the "zig" and "zag" facets stays unchanged. This reassembling process occurs thanks to annihilations of kinks and without characteristic length-scale. Indeed, the averaged size of the domains increases regularly in time. The dynamics, which tends to separate the zig and zag states, looks like the one-dimensional counterpart of the spinodal decomposition dynamics observed in conservative phase transition system [Calisto *et al.*, 2000; Argentina *et al.*, 2005].

For large $\eta > 0$, the model (9) shows a periodic structure in the x-direction, stripe pattern [see Fig. 1(d)], which coexists with the uniform zero state. In this region of parameters, the interface connecting these states is stable and it is motionless in a region of parameters, which corresponds to the pinning range. When η is decreasing, this interface exhibits a spatial instability. For $\eta > 0.12$ the flat interface is stable [see Fig. 1(d)]. For $0 < \eta < 0.12$ the flat interface is transversally unstable, under a small perturbation, the flat interface becomes a periodic interface [see Fig. 1(c)]. Hence, as a consequence of the confluence of transversal instability exhibited by the NWS equation and the interaction of the envelope variation with the small underlying pattern the interface presents a transversal periodic structure. We observe numerically that this interface is motionless in a region of parameters. In [Hilali *et al.*, 1995], a comparable structure has been observed at the interface of super critical bifurcation when a parameter is changed in the longitudinal direction, at variance, the embroidery interface observed in model (9) is a result of a spontaneous spatial breaking of symmetry. Figure 2 shows the amplitude of the embroidery or transversal periodic interface as function of η, it shows that the bifurcation is supercritical and the amplitude is the square root of the bifurcation parameter, that is, the amplitude of embroidery satisfies

$$a = \alpha\sqrt{\eta_c - \eta} \tag{10}$$

where $\alpha = 7.2$ and $\eta_c = 0.12$. Numerical simulations of the Swift–Hohenberg equation show a supercritical bifurcation for the embroidery interfaces. For $0.095 < \eta < 0.12$ these periodic solutions are stable. However, if $\eta < 0.095$ these solutions are unstable too and exhibit a similar zigzag

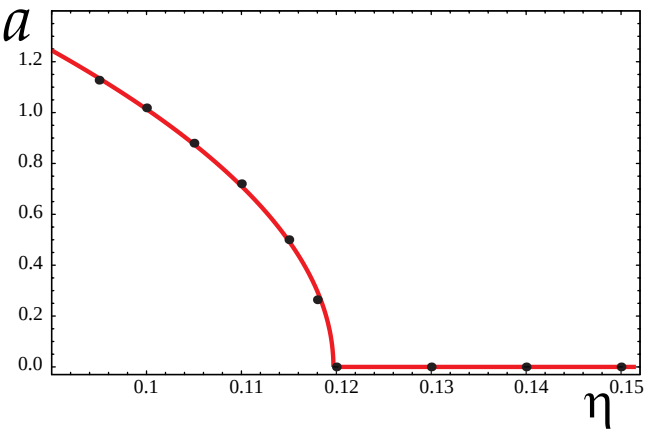

Fig. 2. Bifurcation diagram. "a" represents the amplitude of the periodic pattern at the interface. The points are numerical solution of model (9) for $\epsilon = -3/16$ and the line is the fitting (10).

coarsening dynamics to those exhibited by NWS (4) [see Fig. 1(b)]. However, this zigzag dynamics for large time is frozen — *frozen pattern* [Verdasca *et al.*, 1995] — that is, the reassembling process of the facets is stopped and gives rise to a transversal pattern state. Therefore, the coarsening dynamics exhibited by NWS model (4) is a cross-over dynamics for the ANWS model (9). If η is decreased further, the cross-over time increases due to the fact that more modes with small wave numbers become unstable.

The spectra of Figs. 1(c) and 1(d) depict the spatial bifurcation of the interface that connects the stripe pattern and uniform state.

4. Moving Front at the Interface

To study the dynamics features of stable flat interface, we consider $\eta = 0.2$. From now on, the parameter η will be fixed to this value. From the symmetry $x \to x + 2n\pi/q$, one can deduce if there is a stable interface at x_o-position then there is another at $x_o + 2n\pi/q$, where n is an integer. A front in the transversal direction can be created connecting two of these interfaces, *transversal front*. The inset in Fig. 3 shows a profile of two of these fronts. Notice that the core of transversal front exhibits spatial damping oscillation, which is a consequence of the slowest spatial mode of the flat interface with a well-defined wave number close to q. Since we numerically only consider periodic boundary conditions in the y-direction, there is always more than one transversal front. The velocity of the transversal front depends on the value of ϵ, for some values the

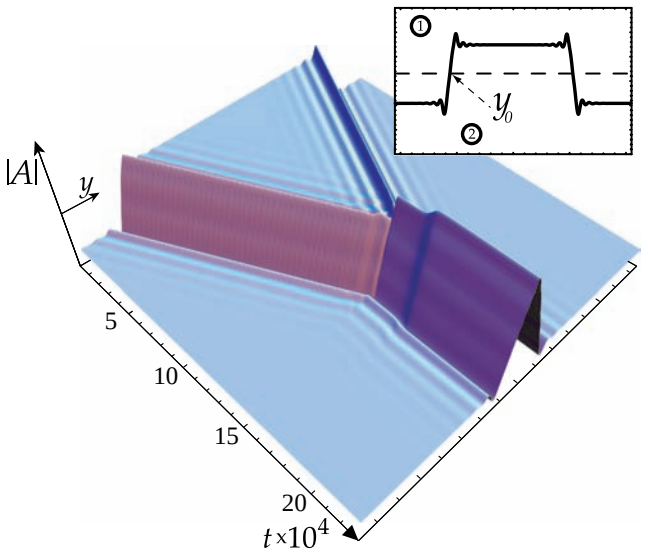

Fig. 3. Spatiotemporal diagram of the interface shown in the inset of model (9) by $\epsilon = -0.186$, $\eta = 0.2$. The interface connects the homogeneous state (1) with the stripe state (2).

front goes to the right or to the left, and for the others the front is motionless. In the one-dimensional systems this front velocity is a consequence of the relative stability between the two states connected by the front. However, in our two-dimensional system, the two states are always equivalent, because one is only the x-direction translation in $2n\pi/q$ to the other. The difference between the two states is that one has more stripes than the other, then the front velocity is a consequence of the relative stability between the stripe pattern and the homogeneous state.

Figure 3 depicts the spatio-temporal evolution of the two transversal fronts. The inset figure shows the transversal interfaces at a given time for $\epsilon = -0.186$. Initially, the fronts are far from each other and the interaction between them is neglected, then the front speed must be the velocity of a single transversal front in an infinity system. When the fronts are nearby, the interaction becomes more and more important. Then the dynamics is mediated by the front interaction. At the end, they arrive at a stable localized state, which is stabilized by the interaction between the fronts [Coullet, 2002; Clerc & Falcon, 2005]. It is important to note that these localized structures are a consequence of the spatial transversal damped oscillation, which generates alternative attractive and repulsive front interaction and then one expects a rich family of localized structures [Clerc *et al.*, 2005a]. The evolution position of the left front is depicted in Fig. 4.

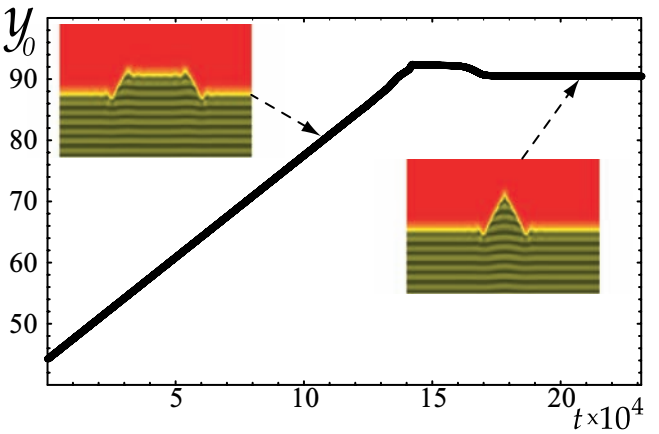

Fig. 4. Position of the left transversal front of model (9) by $\epsilon = -0.186$, $\eta = 0.2$. The inset figures depict the front solutions in the respective given time.

The evolution position of the right front is exactly symmetrical to the left one.

The average speed of the left front is depicted in Fig. 5 for different values of ϵ when the fronts are far from each other. As we have mentioned, the right front speed is minus the left front speed ($\overline{v}_{\text{right}} = -\overline{v}_{\text{left}} = -\overline{v}$). Hence, the velocity of the distance or width between the fronts is minus the double of this velocity ($\dot{\Delta} = -2\,\overline{v}$, where Δ represents the distance between the fronts). Figure 5 shows an interval of zero velocity, which represents stable localized structures, *localized structures range*, around the Maxwell point of the transversal patterns ($\epsilon \approx -0.184$), which is different from the Maxwell point between the stripes and the homogeneous state ($\epsilon = -0.1875$). The localized structures range is $-0.18416 < \epsilon < -0.18374$. For $\epsilon < -0.18416$ the velocity of the left front is

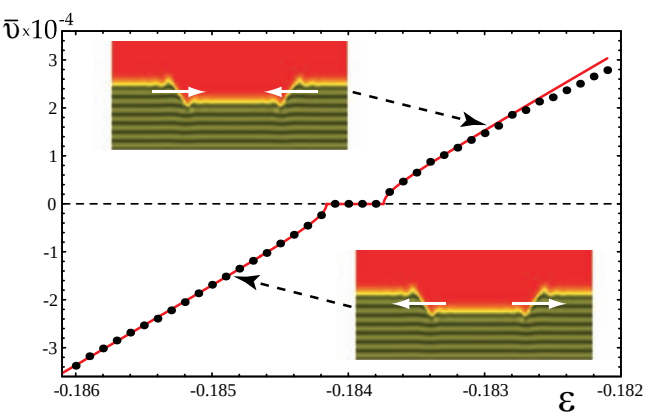

Fig. 5. Transversal front speed for model (9) by $\eta = 0.2$. The continuous lines are the fitting (11). Inset figures stand for transversal front propagation for the respective ϵ parameter.

negative, that means the homogeneous state invades the stripe state. For $\epsilon > -0.18374$ the velocity is positive and the stripe pattern invades the homogeneous state. This process stops when the fronts arrive at the next localized structure range of the smaller localized structure, and if there is no stable localized state for this value of ϵ, the invasion will continue in the orthogonal direction. In Fig. 5 the points are the numerical solution of the model (9) and the continuous line is the fitting

$$\overline{v} = \gamma\,(\epsilon - \epsilon_M)\sqrt{1 - \left(\frac{\epsilon_c}{\epsilon - \epsilon_M}\right)^2}, \qquad (11)$$

obtained from the fronts interaction [Rojas, 2005], where $\gamma = 0.165$, $\epsilon_M = -0.18395$, and $\epsilon_c = 2.1 \times 10^{-4}$. The fitting (11) is in quite good agreement with the numerical results. Because in the pinning range the fronts are stationary, there exists a infinity of localized state of quantized sizes [Clerc & Falcon, 2005].

5. Localized Structures

The previous section shows that there is a region in the parameters space where the fronts interaction gives motionless fronts, the localized structures range. Since the fronts exhibit transversal spatial oscillations at the interface (see inset pictures in Fig. 5), the interaction between the fronts alternate from attractive to repulsive depending on the distance between them. Hence, there is a discrete family of localized structures of quantized sizes [Coullet, 2002]. The first four elements of this family are depicted in Fig. 6 for $\epsilon = -0.184$. Figure 6(a) shows

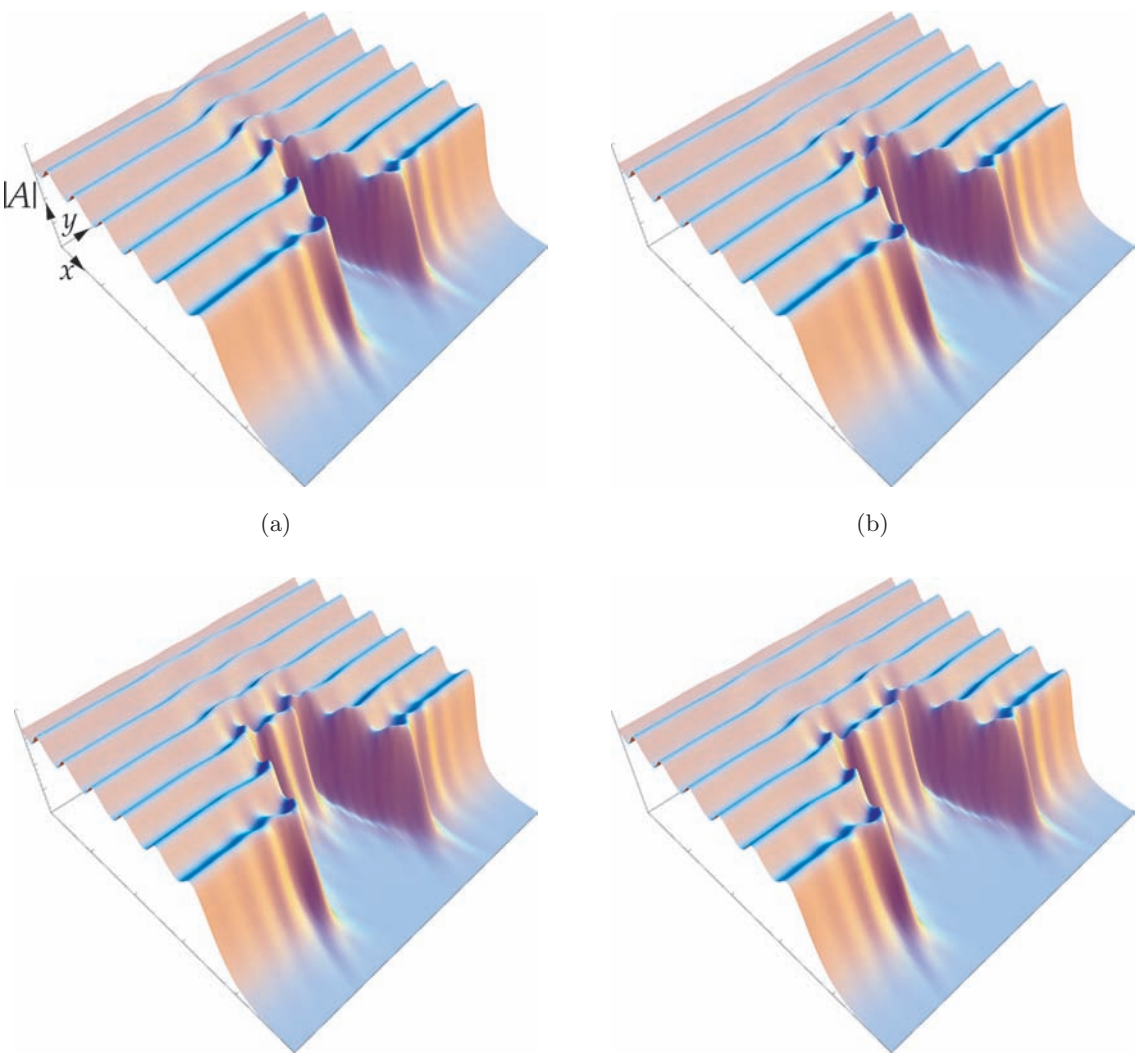

(a) (b) (c) (d)

Fig. 6. Localized states for $\eta = 0.2$ and $\epsilon = -0.184$: (a) $\mathcal{LS}_1$, (b) $\mathcal{LS}_2$, (c) $\mathcal{LS}_3$, and (d) $\mathcal{LS}_4$.

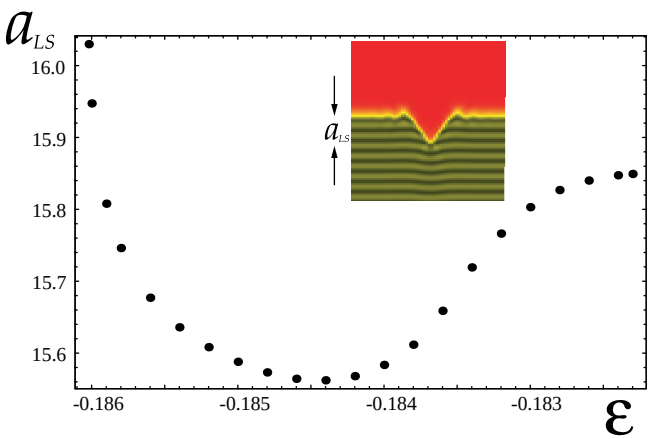

Fig. 7. Amplitude of the localized structure $\mathcal{LS}_1$ for different values of the parameter ϵ with $\eta = 0.2$. The inset figure shows this localized structure and their respective amplitude a_{LS}.

the smallest localized structure of the family which has one oscillation, Figs. 6(b)–6(d) have two, three, and four oscillations respectively. We introduce the following notation, $\mathcal{LS}_n$ stands for the localized structure with n oscillations.

The smallest localized structure $\mathcal{LS}_1$ [Fig. 6(a)] is the most stable in the family, because the interaction between the fronts is the strongest. Almost all the elements in the family only exist in the localized structures range. However, the smallest one has the largest domain, $-0.1861 < \epsilon < -0.1820$. We have defined the amplitude of localized structure (a_{LS}) as the longitudinal distance between the minimum and the asymptotic value of the interface (see inset in Fig. 7). For different values of ϵ in this interval, the amplitude a_{LS} is different, this is shown in

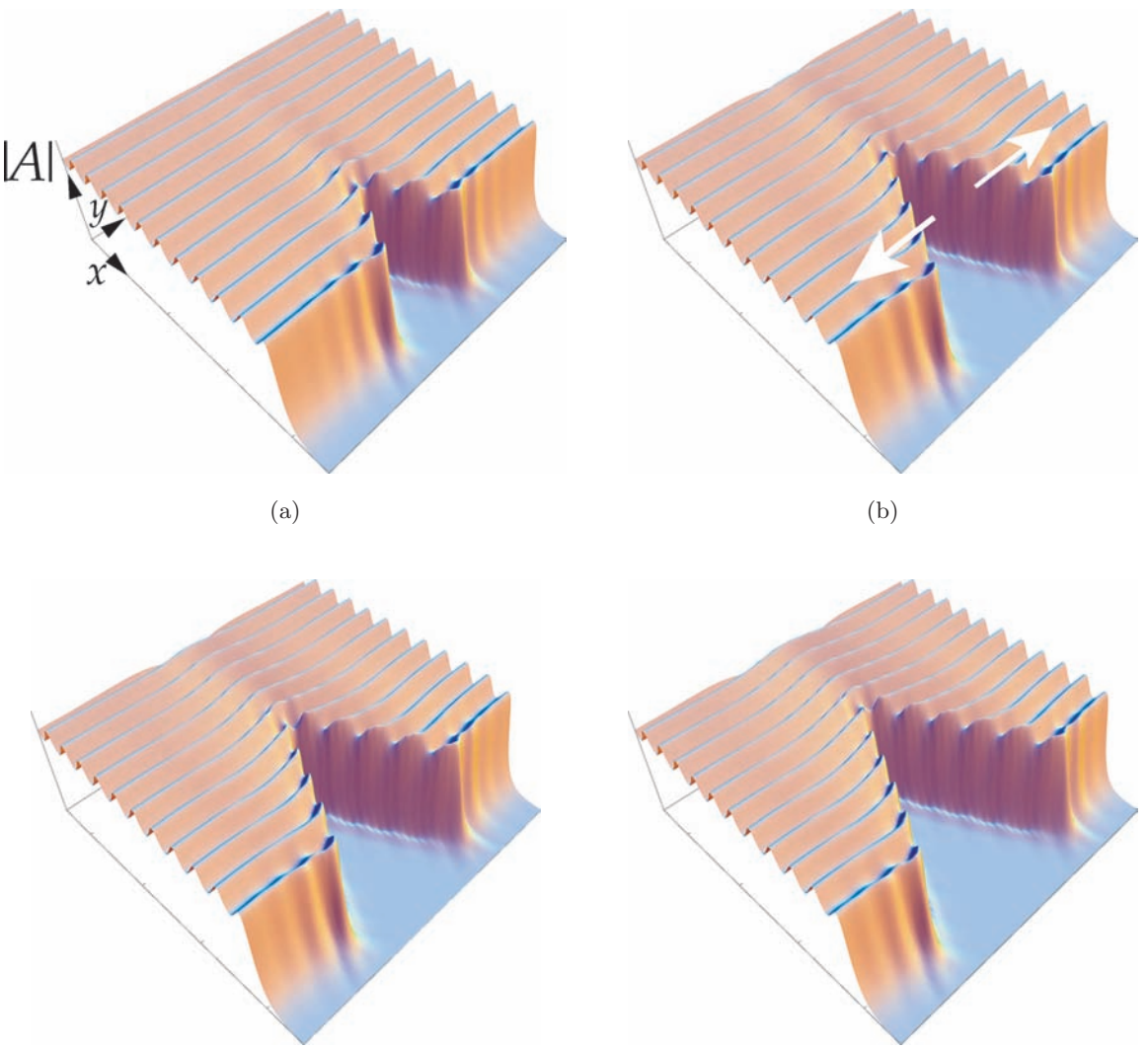

(a) (b)

(c) (d)

Fig. 8. Unstable localized states for $\eta = 0.2$ and $\epsilon = -0.1865$.

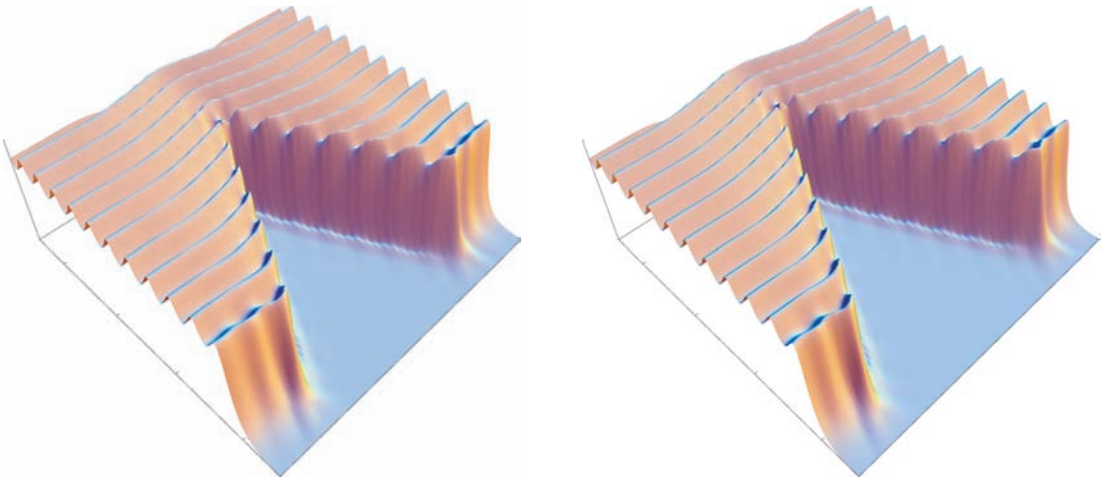

(e) (f)

Fig. 8. (*Continued*)

Fig. 7. Numerically we observe that this amplitude has a minimum for $\epsilon = -0.1844$.

The localized structure $\mathcal{LS}_1$ is unstable outside of the interval $-0.1861 < \epsilon < -0.1820$. Also, Fig. 5 shows that for $\epsilon < -0.18395$ the homogeneous state is more stable than the stripe pattern and for $\epsilon > -0.18395$ the stripe pattern is more stable than the homogeneous state. Then, for $\epsilon < -0.1861$ the localized structure $\mathcal{LS}_1$ is unobserved and the homogeneous state invades the stripe pattern. These remarks are consistent with Fig. 7, which shows a divergence of the amplitude when $\epsilon \to -0.1861$. Figure 8 shows the evolution of this instability for $\epsilon = -0.1865$, which is consistent with the earlier observation: the homogeneous state invades the other state, increasing continuously the amplitude of the localized state $\mathcal{LS}_1$, which is now unstable. The growth of the amplitude is not a straight line, it increases by steps as depicted in Fig. 9. These steps are results of the ghosts of the other localized structures $\mathcal{LS}_1$ [Strogatz, 1994]. It is important to remark that similar wedge type propagation is observed in subcritical Swift–Hohenberg equation.

For $\epsilon > -0.1820$, the localized structure $\mathcal{LS}_1$ is also unobservable. However, the stripe pattern is more stable than the homogeneous state, then the stripe pattern invades the other state. Figure 7 does not reflex this feature, because one expects that the amplitude must decrease continuously when ϵ increases from -0.1861 to -0.1820 and that there is an inflexion point near the respective Maxwell point ($\epsilon_M = -0.18395$). However, this is not the case, Fig. 7 shows that when $\epsilon \to -0.1820$ the amplitude of transversal localized structure increases and the slope goes to zero. This behavior could be a consequence of a saddle-node bifurcation of the localized state. Figure 10 shows the evolution of this instability. We observe that the evolution is governed by the maxima in the transversal interface, they grow continuously invading the homogeneous state. Figure 11 shows the evolution of the maximum of the transversal interface. It is not a straight line again, this evolves by steps which are related to the ghost of the complement localized structures [Strogatz, 1994].

Numerically by changing the initial condition, we observe similar localized structures to those shown in Fig. 6 with a maximum in place of a minimum (Fig. 12). We call this localized structure as *complement localized structure* $\mathcal{LS}_1^c$, because this is

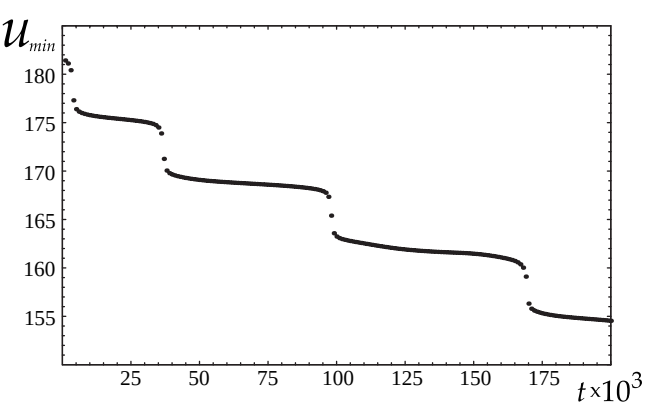

Fig. 9. The position of the minimum of the localized state for model (9) with $\eta = 0.2$ and $\epsilon = -0.1865$.

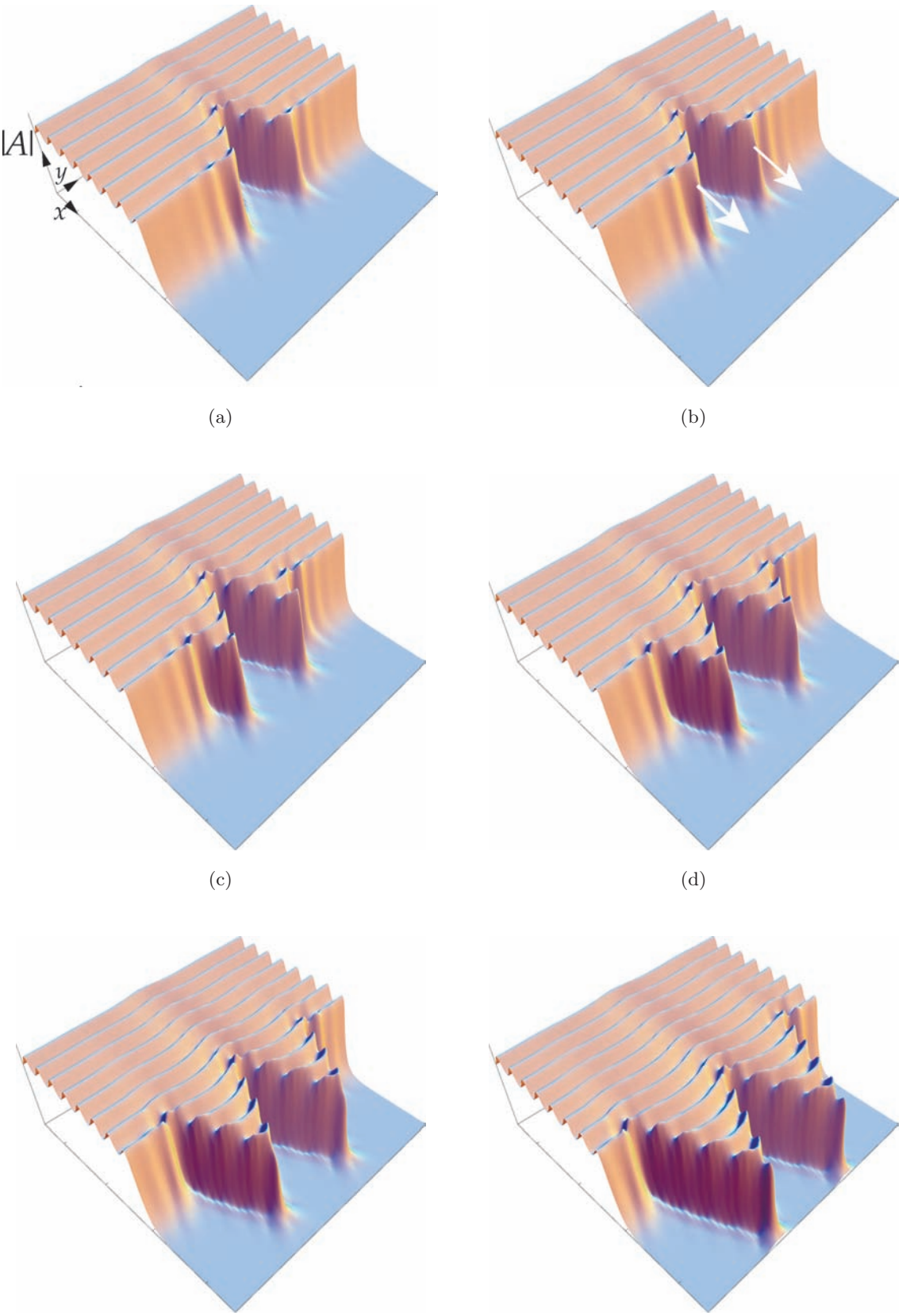

(a) (b)

(c) (d)

(e) (f)

Fig. 10. Unstable localized state for $\eta = 0.2$ and $\epsilon = -0.182$.

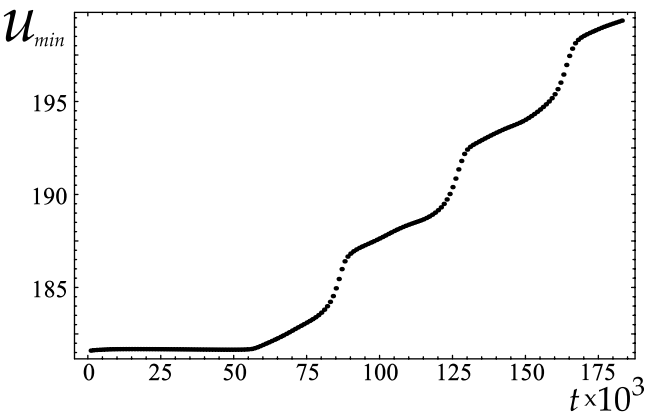

Fig. 11. The position of the minimum of the localized state for model (9) with $\eta = 0.2$ and $\epsilon = -0.1865$.

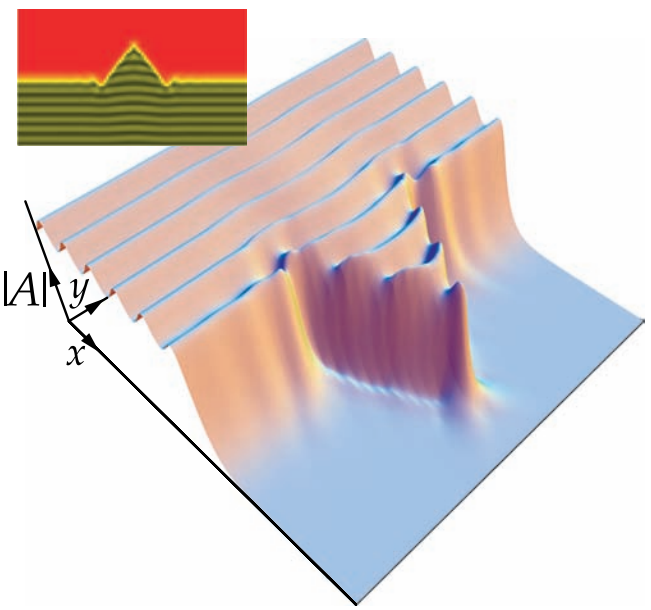

Fig. 12. Localized structure $\mathcal{LS}_1^c$ for $\epsilon = -0.186$ and $\eta = 0.2$.

a simple mirror reflection symmetry of the localized structure $\mathcal{LS}_1$.

6. Conclusions

Systems with coexistence between stable stripe pattern and uniform states can exhibit interfaces connecting these states. Recently in [Clerc *et al.*, 2007], it is shown that in anisotropic systems flat interface linking stripe pattern with uniform state is transversal stable. However, interfaces in isotropic systems can present a wealthy and unexpected transversal dynamics like: spatial instability, embroideries, zigzag instability, front propagation and localized states. In order to clarify the complex dynamics exhibited by these interfaces, we have studied them using a prototype model, the amending Newell–Whitehead–Segel amplitude equation. This model accounts for the complex transversal dynamics at the interface, including front propagations, transversal embroideries, locking phenomena, and transversal localized structures. However, the depinning effect, nucleation of convex–concave disclination pairs and labyrinthic pattern — which has been reported in the supercritical Swift–Hohenberg model [Hagberg *et al.*, 2006] — are not contained in the amended amplitude Swift–Hohenberg equation (9). To describe these rich phenomena the fixed coordinate system x, y used in Eq. (9) must be promoted to the local direction of the stripe pattern and change the sign of high nonlinearity in order to describe the dynamics observed in the bent stripe. Work in this direction is in progress.

Acknowledgments

The authors thank D. Asenjo for useful discussions. The simulation software *DimX* developed at INLN, France, has been used for all the numerical simulations. The authors acknowledge the support of Programa Anillo ACT 15 of *Programa Bicentenario de Ciencia y Tecnología* of the Chilean government. M. G. Clerc thanks the support of FONDAP grant 11980002. R. Rojas thanks the financial support of Fondecyt 3070039.

References

Aranson, I. S., Malomed, B. A., Pismen, L. M. & Tsimring, L. S. [2000] "Crystallization kinetics and self-induced pinning in cellular patterns," *Phys. Rev. E* **62**, R5–R8.

Argentina, M., Clerc, M. G., Rojas, R. & Tirapegui, E. [2005] "Coarsening dynamics of the one-dimensional Cahn–Hilliard model," *Phys. Rev. E* **71**, 046210–046224.

Bensimon, D., Shraiman, B. I. & Croquette, V. [1988] "Nonadiabatic effects in convection," *Phys. Rev. A* **38**, 5461–5464.

Bortolozzo, U., Rojas, R. & Residori, S. [2005] "Spontaneous nucleation of localized peaks in a multistable nonlinear system," *Phys. Rev. E* **72**, 045201(R).

Bortolozzo, U., Clerc, M. G., Falcon, C., Residori, S. & Rojas R. [2006] "Localized states in bistable pattern-forming systems," *Phys. Rev. Lett.* **96**, 214501.

Burke, J. & Knobloch, E. [2006] "Localized states in the generalized Swift–Hohenberg equation," *Phys. Rev. E* **73**, 056211.

Burke, J. & Knobloch, E. [2007] "Homoclinic snaking: Structure and stability," *Chaos* **17**, 037102.

Calisto, H., Clerc, M. G., Rojas, R. & Tirapegui, E. [2000] "Bubbles interactions in the Cahn–Hilliard equation," *Phys. Rev. Lett.* **85**, 3805–3808.

Chevallard, C., Clerc, M., Coullet, P. & Gilli, J. M. [2002] "Zig-zag instability of an Ising wall in liquid crystals," *Europhys. Lett.* **58**, 686–692.

Clerc, M. G. & Falcon, C. [2005] "Localized patterns and hole solutions in one-dimensional extended systems," *Physica A* **356**, 48–53.

Clerc, M. G., Escaff, D. & Kenkre, E. [2005a] "Patterns and localized structures in population dynamics," *Phys. Rev. E* **72**, 056217.

Clerc, M. G., Falcon, C. & Tirapegui, E. [2005b] "Additive noise induces front propagation," *Phys. Rev. Lett.* **94**, 148302.

Clerc, M. G., Falcon, C., Escaff, D. & Tirapegui, E. [2007] "Noise induced rolls propagation," *Eur. Phys. J. Spec. Top.* **143**, 171–179.

Clerc, M. G., Escaff, D. & Rojas, R. [2008] "Transversal interface dynamics of a front connecting a stripe pattern to a uniform state," *Europhys. Lett.* **83**, 28002.

Coullet, P. [2002] "Localized patterns and fronts in nonequilibrium systems," *Int. J. Bifurcation and Chaos* **12**, 2445–2457.

Cross, M. C. & Hohenberg, P. C. [1993] "Pattern formation outside of equilibrium," *Rev. Mod. Phys.* **65**, 851–1112.

Elphick, C., Tirapegui, E., Brachet, M. E., Coullet, P. & Iooss, G. [1987] "A simple global characterization for normal forms of singular vector fields," *Physica D* **29**, 95–127.

Goldstein, R. E., Gunaratne, G. & Gil, L. [1990] "Defects and travelling-wave states in nonequilibriumpatterns with broken parity," *Phys. Rev. E* **41**, 5731–5734.

Hagberg, A., Yochelis, A., Yizhaq, H., Elphick, C., Pismen, L. & Meron, E. [2006] "Linear and nonlinear front instabilities in bistable systems," *Physica D* **217**, 186–192.

Hilali, M. F., Métens, S., Borckmans, P. & Dewel, G. [1995] "Pattern selection in the generalized Swift–Hohenberg model," *Phys. Rev. E* **51**, 2046–2052.

Jakobsen, P. K., Lega, J., Feng, Q., Staley, M., Moloney, J. V. & Newell, A. C. [1994] "Nonlinear transverse modes of large-aspect-ratio homogeneously broadened lasers: I. Analysis and numerical simulation," *Phys. Rev. A* **49**, 4189–4200.

Kozyreff, G. & Chapman, S. J. [2006] "Asymptotics of large bound states of localized structures," *Phys. Rev. Lett.* **97**, 044502.

Landau, L. D. [1944] "On the problem of turbulence," *C. R. Acad. Sci. URSS* **44**, 311–315.

Malomed, B. A., Nepomnyashchy, A. A. & Tribelsky, M. I. [1990] "Domain boundaries in convection patterns," *Phys. Rev. A* **42**, 7244–7263.

Murray, J. D. [1993] *Mathematical Biology* (Springer-Verlag, Berlin).

Newell, A. C. & Whitehead, J. A. [1969] "Finite bandwidth, finite amplitude convection," *J. Fluid Mech.* **38**, 279–303.

Newell, A. C. & Whitehead, J. A. [1971] "Review of the finite bandwidth concept," *Instability of Continuous Systems*, ed. Leipholz, H. (Springer-Verlag, NY), pp. 284–289.

Newell, A. C., Passot, T. & Lega, J. [1993] "Order parameter equation for patterns," *Ann. Rev. Fluid Mech.* **25**, 399–453.

Nicolis, G. & Prigogine, I. [1977] *Self-Organization in Nonequilibrium Systems: From Dissipative Structures to Order Through Fluctuations* (John Wiley & Sons).

Pomeau, Y. [1986] "Front motion, metastability and subcritical bifurcation in hydrodynamics," *Physica D* **23**, 3–11.

Rojas, R. [2005] "Sur de Gouttes, Cristaux Liquides et Fronts," PhD Thesis at University of Nice-Sophia Antipolis, France (http://tel.archives-ouvertes.fr/).

Sakaguchi, H. & Brand, H. R. [1996] "Stable localized solutions of arbitrary length for the quintic Swift–Hohenberg equation," *Physica D* **97**, 274–285.

Schlüter, A., Lortz, D. & Busse, F. H. [1965] "On the stability of steady finite amplitude convection," *J. Fluid Mech.* **23**, 129–144.

Segel, L. A. [1969] "Distant sidewalls cause slow amplitude modulation of cellular convection," *J. Fluid Mech.* **38**, 203–224.

Strogatz, S. H. [1994] *Nonlinear Dynamics and Chaos* (Perseus Books Group).

Stuart, J. T. [1960] "On the non-linear mechanics of wave disturbances in stable and unstable parallel flows Part 1. The basic behaviour in plane Poiseuille flow," *J. Fluid Mech.* **9**, 353–370.

van Hecke, M., Hohenberg, P. C. & van Saarloos, W. [1994] "Amplitude equations for patterns forming systems," in *Fundamental Problems in Statistical Mechanics VIII.* eds. van Beijeren, H. & Ernst, M. H. (North-Holland, Amsterdam).

van Saarloos, W. & Hohenberg, [1992] "Fronts, pulses, sources and sinks in generalized complex Ginzburg–Landau equations," *Physica D* **56**, 303–367.

Verdasca, J., Borckmans, P. & Dewel, G. [1995] "Chemically frozen phase separation in an adsorbed layer," *Phys. Rev. E* **52**, R4616–R4619.

Walgraef, D. [1996] *Spatio-Temporal Pattern Formation, with Examples in Physics, Chemistry and Materials Science* (Springer-Verlag, NY).